

# Modiff: Action-Conditioned 3D Motion Generation with Denoising Diffusion Probabilistic Models

Mengyi Zhao, Mengyuan Liu, Bin Ren, Shuling Dai, and Nicu Sebe

**Abstract**—Diffusion-based generative models have recently emerged as powerful solutions for high-quality synthesis in multiple domains. Leveraging the bidirectional Markov chains, diffusion probabilistic models generate samples by inferring the reversed Markov chain based on the learned distribution mapping at the forward diffusion process. In this work, we propose Modiff, a conditional paradigm that benefits from the denoising diffusion probabilistic model (DDPM) to tackle the problem of realistic and diverse action-conditioned 3D skeleton-based motion generation. We are a pioneering attempt that uses DDPM to synthesize a variable number of motion sequences conditioned on a categorical action. We evaluate our approach on the large-scale NTU RGB+D dataset and show improvements over state-of-the-art motion generation methods.

**Index Terms**—Motion Generation, Diffusion Model, Skeleton Data, Conditional Motion Generation, Generative Model

## I. INTRODUCTION

Generating realistic human motions is essential for human behavior understanding, since it can be applied for numerous applications including animation [1], virtual or augmented reality [2], [3], as well as data-driven deep learning [4], [5], [6], [7]. Despite the substantial progress made in modeling human dynamics, synthesizing natural, diverse, and controllable pose sequences remains challenging due to the complicated inter- and intra-class variations [5]. Motion synthesis methods can be roughly divided into two categories: 1) unconditioned generation [8], [5] and 2) conditioned synthesis with the condition coming from various modalities *i.e.*, music [9], speech [10], [11], emotion [12], pre-defined action categories [13], [14], text prompts [15], [2], past and/or future pose [16], [17], [18]. In this paper, we focus on the conditioned generation case, aiming to generate more diverse 3D skeleton-based motion sequences in a controllable manner.

During the past decades, generative models for human motion generation have been investigating widely [19], [13], [20]. As a result, numerical methods were proposed based on Generative Adversarial Networks (GANs) [19], [20], [17],

[21], Variational Auto Encoder (VAE) [22], [16], [13], [2], Neural Distance Fields (NDF) [23], [24], [14] or diffusion models [25], [26], [27], [28], [29]. Generally, realism and diversity are two crucial aspects for evaluating the quality of the motion generation task. To maintain diversity and boost realism during high-quality sampling, many approaches introduce GANs [30] to motion modality since GANs already showed remarkable success in image synthesizing. For instance, prior works [19] and [20] treated the predictor as a conditional generator and train the model in an adversarial manner with customized discriminators designed for human motion generation. Moreover, Harvey *et al.*[17] modified motion predictors into transition generators to tackle the in-between task, especially for variable-length complement given sparse key frames of animation.

To produce a diverse set of possible future poses, Yuan *et al.* [16] proposed a new sampling strategy by exploiting conditional variational autoencoder (CVAE) [31] and KL constraints to balance between diversity and likelihood. Petrovich *et al.* [13] first designed a Transformer-based CVAE for action-conditioned motion generation, namely ACTOR, which generates motions by sampling from the latent space based on parametric SMPL [32] model. More recently, they further extended ACTOR to text-conditioned motion generation [2] by learning a joint latent space of two modalities *i.e.*, motion and text based on a VAE framework.

The recent success of Neural Fields has attracted large interest in the computer vision community due to their effective capacity of representing complex data. Peng *et al.* [23] presented an implicit neural representation for dynamic humans for the new-view RGB video synthesis and 3D human model reconstruction. Unlike VAE-based approaches that infer variational distributions with an encoder, Cervantes *et al.*[14] proposed a model for action-conditional human motion generation that exploits variational Implicit Neural Representations (INR). In particular, their INR-based framework ensures sample-level representation optimization and enables variable-length sequence generation. Tiwari *et al.* [24] proposed to learn a human action prior that models the manifold of possible human poses represented by a scalar neural distance field, and employed this prior to downstream tasks *i.e.*, denoising mocap data, occlusion data recovery, and 3D reconstruction from images. As a result, their formalism can project the human poses to a pose manifold instead of the Gaussian distribution that is commonly adopted in the VAE-based methods. This leads to a distance-preserving representation between poses.

More recently, the diffusion model has shown its effectiveness in image synthesis [33], [34], [35]. Followed by these

M. Zhao is with the State Key Laboratory of Virtual Reality Technology and Systems, Beihang University, Beijing 100191, China (e-mail: zhaomengyi@buaa.edu.cn).

Mengyuan Liu is with the School of Intelligent Systems Engineering, Sun Yatsen University, Shenzhen 510275, China, and also with Guangdong Provincial Key Laboratory of Fire Science and Technology, Guanzhou 510006, China (e-mail: liumy85@mail.sysu.edu.cn).

B. Ren is with University of Pisa & University of Trento, Italy (e-mail: bin.ren@unitn.it).

S. Dai is with the State Key Laboratory of Virtual Reality Technology and Systems, Beihang University, Beijing 100191, China, and also with Jiangxi Research Institute, Beihang University, China (e-mail: sldai@buaa.edu.cn).

N. Sebe is with University of Trento, Trento, Italy (e-mail: niculae.sebe@unitn.it).

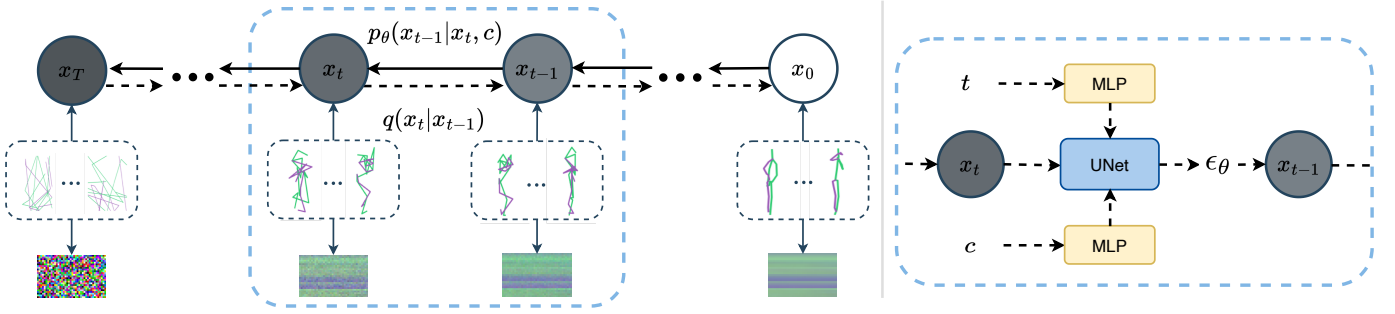


Fig. 1. **Overview of Modiff.** The **diffusion** and **reverse** processes are represented by the solid and dashed arrows in the left part, respectively. During the reverse process, the detailed denoising procedure is exhibited in the right part. Note that, as shown in the bottom part, we treat the 3D skeleton sequence as a 2D image during training, and we also convert the sampled skeleton sequences into images to have a quick glance at the sampling results.

advances, several works have explored the capacity of the diffusion model for the human motion field [25], [28], [29]. These works investigated text-to-motion generation with a Transformer-based diffusion model on a large-scale dataset HumanML3D [36]. However, based on the observation of the generated results from the corresponding official implementation of [29], we identify two limitations, *i.e.*, 1) When an input text involves multiple actions, the generated sequences may fail to combine the corresponding actions properly or produce tangled motions with other unrelated actions. 2) Given a textual description with high-level semantic information *e.g.*, “A person jumps up and down for two times”, their model generates incorrect actions, which means their model is not aware of the actual meaning of “two times”. In addition, Findlay *et al.* [27] employed DDPM [33] for styled walking generation. Meanwhile, Saadatnejad *et al.* [37] introduced a framework for 3D human pose forecasting. It can produce future sequences recursively and incorporate denoising and post-processing by fully-exploit the properties of the diffusion model. However, their method is not an end-to-end paradigm, which increases the complexity of the task. For conditional action generation, [28], [29] applied their framework on the HumanAct12 and UESTC datasets, which contain 12 and 40 action classes, respectively. But for more challenging scenarios *e.g.*, having more action categories to learn, the state-of-the-art approach is a GAN-based method *i.e.* Kinetic-GAN [38], which leverages GANs and Graph Convolutional Networks (GCNs) to generate human action sequences conditioned on the class label from Gaussian noise.

In this work, inspired by the diffusion model in image synthesis which outperforms GANs [35], we aim to explore the effectiveness of diffusion models on sequential skeleton-based motion generation. In particular, we focus on the problem of how to represent a 3D skeleton sequence and exploit the DDPM controlled by an action label. Conclusively, our goal is to take a pre-defined action label *e.g.*, “jump up” as input and generate an arbitrary number of plausible 3D human motion sequences via diffusion model. In concentrate, our contribution is a conditional diffusion model-based motion generation framework. Specifically, we first treat the skeleton sequence as a 2D image matrix with 3 channels, then inject the label guidance into each reverse step during training and sampling. Finally, we evaluate our method on the challenging

NTU RGB+D dataset with 60 action classes and the NTU RGB+D two-person dataset with 11 interaction classes. The experimental results show the proposed Modiff achieves state-of-the-art performances on both datasets.

## II. DIFFUSION MODEL FOR 3D SKELETON-BASED MOTION GENERATION

In this work, our goal is to tackle the task of action-conditioned 3D skeleton-based human motion generation. Formally, given an action label  $c \in \mathcal{C}$ , where  $\mathcal{C}$  is a predefined category set, we aim to generate arbitrary *i.e.*,  $N$  sequences of body poses  $x_{1:f}^N$  with  $f$  frames. In our case, each pose  $x_i \in \mathbb{R}^{3 \times J}$  corresponds to an articulated human body, *i.e.*, the 3D coordinates of human joints, where  $J$  represents the number of joints. We use  $x$  as a shorthand for each motion sequence  $x_{1:f}$ . Hence, our motion diffusion process operates on a sequence level.

### A. Denoising diffusion probabilistic model

As shown in Figure 1, diffusion model[39] is composed of two mapping processes using the Markov chain. Each process essentially converts one distribution *e.g.*, Gaussian into another *e.g.*, motion data. According to the starting and endpoint of Markov chains, the two processes are named forward diffusion process for the inference and reverse diffusion process for the generation.

Given the real (motion) data drawn from the distribution  $x_0 \sim q(x_0)$  with dimension  $D$ , the *diffusion process* is producing the latent  $x_t \in \mathbb{R}^D$  by adding Gaussian noise to the data progressively at time  $t \in \{1, \dots, T\}$ :

$$\begin{aligned}
 q(x_{0:T}) &:= q(x_0) \prod_{t=1}^T q(x_t | x_{t-1}), \\
 q(x_{1:T} | x_0) &:= \prod_{t=1}^T q(x_t | x_{t-1}), \\
 q(x_t | x_{t-1}) &:= \mathcal{N}(x_t; \sqrt{1 - \beta_t}x_{t-1}, \beta_t \mathbf{I}),
 \end{aligned} \tag{1}$$

where  $\beta_t \in (0, 1)$  is the variance of Gaussian noise. Symmetrically, the *reverse process* is as follows:

$$\begin{aligned}
 p_\theta(x_{0:T}) &:= p(x_T) \prod_{t=1}^T p_\theta(x_{t-1} | x_t), \\
 p_\theta(x_{t-1} | x_t) &:= \mathcal{N}(x_{t-1}; \mu_\theta(x_t, t), \Sigma_\theta(x_t, t)),
 \end{aligned} \tag{2}$$

---

**Algorithm 1** Action-conditioned Sampling Algorithm
 

---

**Input:** Action label  $c$ , learned  $\epsilon_\theta(x_t, t, c)$ 
**Output:** Motion sequence  $x_0$ 

- 1:  $x_T \leftarrow$  sample from  $p(x_T) = \mathcal{N}(0, \mathbf{I})$
  - 2: **for**  $t = T, T-1, \dots, 1$  **do**
  - 3:  $\mu_\theta(x_t, t, c) \leftarrow$  calculate from the learned  $\epsilon_\theta(x_t, t, c)$  using Eq.7
  - 4:  $x_{t-1} \leftarrow$  sample from  $\mathcal{N}(x_{t-1}; \mu_\theta(x_t, t, c), \sigma_t^2 \mathbf{I})$
  - 5: **end for**
  - 6: **return**  $x_0$
- 

where  $p(x_T) = \mathcal{N}(0, \mathbf{I})$ . Notably, this posterior can be used to generate sample  $x_0$  given a Gaussian noise  $x_T \sim \mathcal{N}(0, \mathbf{I})$  and reducing the noise gradually from time step  $T$  to 0. Moreover,  $\mu_\theta$  and  $\Sigma_\theta$  are derived from the diffusion step  $t$  and latent  $x_t$ , which describe the learned Gaussian transition by the model after training to remove the Gaussian noise from  $x_t$  to  $x_{t-1}$ . Thus, sample  $x_{t-1} \sim p_\theta(x_{t-1} | x_t)$  is to calculate:

$$x_{t-1} = \frac{1}{\sqrt{\alpha_t}} \left( x_t - \frac{\beta_t}{\sqrt{1-\alpha_t}} \epsilon_\theta(x_t, t) \right) + \sigma_t \mathbf{z}, \quad (3)$$

where  $\mathbf{z} \sim \mathcal{N}(0, \mathbf{I})$  and  $\sigma_t \approx \sqrt{\beta_t}$ , which means  $\Sigma_\theta(x_t, t) = \sigma_t^2 \mathbf{I}$  is fixed to a constant.

During the training phase, [33] proposed to sample latent  $x_t$  from arbitrary step  $t$  with  $x_0$ . To be specific, we sample step  $t \sim [1, T]$  from a uniform distribution and get intermediate  $x_t$  from  $q(x_t | x_0)$  as follows:

$$q(x_t | x_0) = \mathcal{N}(x_t; \sqrt{\bar{\alpha}_t} x_0, (1 - \bar{\alpha}_t) \mathbf{I}), \quad (4)$$

$$x_t = \sqrt{\bar{\alpha}_t} x_0 + \sqrt{1 - \bar{\alpha}_t} \epsilon$$

where  $\bar{\alpha}_t = \prod_{m=0}^t \alpha_m$  and  $\alpha_t = 1 - \beta_t$ ,  $\epsilon \sim \mathcal{N}(0, \mathbf{I})$ . While [34] found that the linear noise schedule is not suitable for low-resolution images, since skeleton data is rather spatially-sparse which can be treated as low-resolution images, we adopt the noise schedule in [34]:

$$\bar{\alpha}_t = \frac{f(t)}{f(0)}, \quad f(t) = \cos \left( \frac{t/T + m}{1 + m} \cdot \frac{\pi}{2} \right)^2, \quad (5)$$

where  $s = 0.008$ . Hence,  $\beta_t = 1 - \frac{\bar{\alpha}_t}{\bar{\alpha}_{t-1}}$ . We feed  $t$  and  $x_t$  to a U-Net[40] model as [33], and predict the  $\epsilon_\theta$  by minimizing the L1 loss experimentally:

$$L_{\text{noise}} = E_{t, x_0, \epsilon} [|\epsilon - \epsilon_\theta(x_t, t)|]. \quad (6)$$

Therefore,  $\mu_\theta(x_t, t)$  can be derived from  $\epsilon_\theta(x_t, t)$  as:

$$\mu_\theta(x_t, t) = \frac{1}{\sqrt{\alpha_t}} \left( x_t - \frac{\beta_t}{\sqrt{1-\alpha_t}} \epsilon_\theta(x_t, t) \right). \quad (7)$$

### B. Action-conditioned diffusion

We leverage a classifier-free diffusion [41] for action-conditioned motion generation, which means no extra classifier is required at the training stage. The label of action class  $c$  is added in the denoising process, which is formulated as:

$$p_\theta(x_{t-1} | x_t, c) := \mathcal{N}(x_{t-1}; \mu_\theta(x_t, t, c), \Sigma_\theta(x_t, t, c)). \quad (8)$$

TABLE I

THE RESULTS OF OUR MODIFF ON THE NTU RGB+D DATASET. WE COMPARE OUR MODEL WITH KINETIC-GAN [38] ON CROSS-SUBJECT BENCHMARK. (BEST RESULTS IN BOLD)

Method	FMD↓	Diversity↑	Multimodality↑
Real	0.39±0.00	36.90±0.13	26.79±0.04
Kinetic-GAN-MLP8 [38]	82.88±8.14	4.47±0.12	3.97±0.07
Kinetic-GAN-MLP4 [38]	9.99±2.31	12.83±0.20	11.04±0.09
Modiff (Ours)	<b>9.12±0.00</b>	<b>12.85±0.19</b>	<b>11.48±0.08</b>

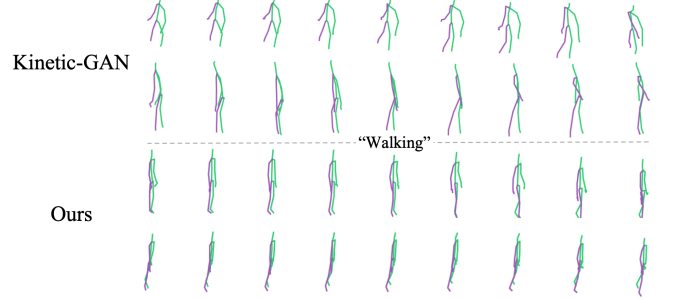


Fig. 2. Visualization of generated motion sequence from Kinetic-GAN [38] and Ours by given label “Walking” on the NTU RGB+D dataset.

In the implementation, we inject class prior by adding a class embedding in the same way as the time step [34] as described in Figure 1. The summary of the sampling algorithms for action-conditioned diffusion is given in Algorithm 1.

## III. EXPERIMENTS

### A. Datasets & Settings

**NTU RGB+D dataset [42].** This is a widely used dataset for skeleton-based action recognition with 3D skeleton annotations. It is composed of 56,880 training samples for 60 action classes which are collected from 40 human subjects.

**NTU RGB+D two-person dataset [42].** We use 11 categories which contain the interactions of two people *e.g.*, “Kicking”, “Hugging” and “Pushing” for state-of-the-art comparison.

**Evaluation metrics.** We evaluate our method on the cross-subject benchmark. This dataset is divided into two subsets according to the IDs of subjects. Consequently, the training set contains 40,320 action sequences, and the testing set contains 16,560 action sequences. To evaluate the quantity of generated motion sequence, we adopt Fréchet Motion Distance (FMD) proposed in [43] as a quantitative metric for computing the distance between the two feature distributions of the real and generated motion samples. We also follow [13], measure the overall diversity and intra-class diversity (denoted as multimodality). Our method is implemented with PyTorch framework and is trained for 100 epochs using the Adam optimizer [44] on one Nvidia RTX A6000 GPU. Before training, we uniform the 3D coordinates of human joints during preprocessing.

### B. Comparison with State-of-the-art Methods

In Table I, we compare our method with the previous state-of-the-art approach Kinetic-GAN [38]. We report the data by

TABLE II  
THE RESULTS OF OUR MODIFF ON THE NTU RGB+D TWO-PERSON DATASET. WE COMPARE OUR MODEL WITH KINETIC-GAN\* [38] ON CROSS-SUBJECT BENCHMARK. (BEST RESULTS IN BOLD)

Method	FMD↓	Diversity↑	Multimodality↑
Real	1.79±0.00	22.65±0.21	20.72±0.23
Kinetic-GAN* [38]	140.49±0.00	5.04±0.03	4.62±0.08
Modiff (Ours)	<b>76.00±0.57</b>	<b>21.75±0.15</b>	<b>19.69±0.52</b>

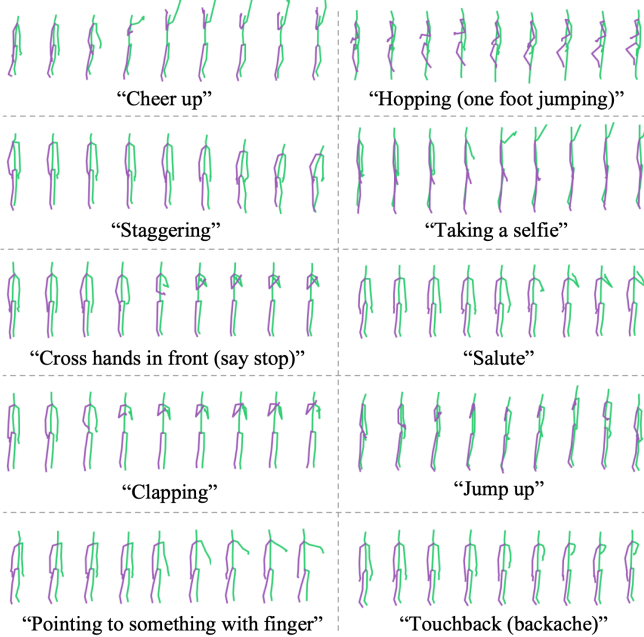


Fig. 3. Visualization of generated motion sequences of our method on the NTU RGB+D dataset. (Best viewed when zoomed in)

using their pre-trained models with released code for a fair comparison. Our results outperform Kinetic-GAN across all types of metrics including FMD, Diversity, and Multimodality. Note that, our presented method is far better than Kinetic-GAN-MLP8 in terms of mean FMD (9.89 vs 82.88). In Table II, we adapt the code of Kinetic-GAN [38] for two-person action generation with slight modification, denoted as Kinetic-GAN\*. Our presented method clearly surpasses Kinetic-GAN\* on all the metrics. In particular, we achieve samples with lower FMD, which is 64.49 less than Kinetic-GAN\*.

We further illustrate the comparison of qualitative results in Figure 2 between kinetic-GAN and ours on “Walking”. We sampled the same number of sequences from ours and kinetic-GAN and choose the best two for comparison. The first motion sequence produced by kinetic-GAN has almost no walking movement, the synthesized person just stands still with the left arm and leg moving slightly over the time span. Also, the second sample shows an unrealistic human motion dynamic, which swaps the left and right part of the body and almost without alternate footsteps. By contrast, our results are more robust and diverse in the rhythm of paces. Although our Modiff shows the promising performance of generating sequential motion samples conditioned on the action type, it still has limitations. 1) Similar to Kinetic-GAN [38], ACTOR [13], and other action-conditioned generation methods, the joints

TABLE III  
ABLATION STUDY RESULTS OF U-NET, LOSS, AND LABEL EMBEDDING.

	Label emb.[29]	Label emb.[34]	L2 loss	L1 loss	U-Net-16	U-Net-32	U-Net-64	FMD↓
B1	✓		✓		✓			161.44±0.31
B2	✓		✓			✓		29.11±0.42
B3	✓		✓				✓	15.70±1.23
B4	✓			✓			✓	9.42±0.00
B5		✓		✓			✓	<b>9.12±0.00</b>
B6		✓	✓				✓	14.34±0.31

in the produced motion sequence may exist jitters over time. 2) Similar to Kinetic-GAN [38], a small portion of sampling results may crash from the beginning or crash at the end.

### C. Ablation Study

We provide the qualitative results in Figure 3 on a bunch of action types, including “Cheer up”, “Hopping”, “Taking a selfie”, “Staggering”, etc. As seen in the generated samples, our method can capture the underlying pattern of predefined actions and produce a realistic sequence with representative keyframes. For instance, one can easily recognize the “Salute” action according to the synthesized movement of raising one hand and placing it next to the ear. Similarly, it’s also intuitive for the “Cross hands in front” sample when we see the generated person cross hands over the chest.

**Effect of U-Net.** Moreover, as illustrated in Table III, we offer the quantitative results of U-Net with different dimensions of latent layers. U-Net-16 means for up and down layers, the minimum dimension is 16, the same as the U-Net-32 and U-Net-64. Intuitively, comparing baseline B3 with B1 and B2, U-Net with higher dimension layers leads to effective latent representation for motion data and achieves better generation results. B3 outperforms B1 and B2 by a large margin on FMD, which decrease FMD metric by 145.74.

**Effect of Loss.** As observed in Table III, we also report the quantitative results of different losses. According to the results of metrics from baseline B3, B4, B5, and B6, L1 loss results in an improvement of 6.28 (B3 vs B4) and 5.22 (B5 vs B6) on FMD metric.

**Effect of Label embedding.** As indicated in Table III, we investigate two different ways of label embedding. Label emb.[34] means the method introduced in Section II-B, Label emb. [29] means the approach used in [29]. By comparing baseline B4 with B5 (our Modiff), Label emb.[34] further boosts the performance of our Modiff by 0.3 on FMD.

## IV. CONCLUSION

This work introduces Modiff, a novel framework based on the diffusion probabilistic model for action-conditioned motion generation. More specifically, the presented Modiff integrates the denoising diffusion model with motion representations, injecting the action-type condition to the reverse Markov chain for action-conditioned motion synthesis. We conducted extensive experiments on a large-scale NTU RGB+D dataset and achieved competitive qualitative and quantitative results compared to the state-of-the-art motion generation method.

## REFERENCES

- [1] S. Starke, Y. Zhao, F. Zinno, and T. Komura, "Neural animation layering for synthesizing martial arts movements," *ACM Transactions on Graphics (TOG)*, vol. 40, no. 4, pp. 1–16, 2021.
- [2] M. Petrovich, M. J. Black, and G. Varol, "Temos: Generating diverse human motions from textual descriptions," *arXiv preprint arXiv:2204.14109*, 2022.
- [3] Y. Zhang and S. Tang, "The wanderings of odysseus in 3d scenes," in *Proceedings of the IEEE/CVF Conference on Computer Vision and Pattern Recognition*, 2022, pp. 20 481–20 491.
- [4] F. Meng, H. Liu, Y. Liang, J. Tu, and M. Liu, "Sample fusion network: An end-to-end data augmentation network for skeleton-based human action recognition," *IEEE Transactions on Image Processing*, vol. 28, no. 11, pp. 5281–5295, 2019.
- [5] R. Zhao, H. Su, and Q. Ji, "Bayesian adversarial human motion synthesis," in *Proceedings of the IEEE/CVF Conference on Computer Vision and Pattern Recognition*, 2020, pp. 6225–6234.
- [6] M. Liu, H. Liu, and C. Chen, "Enhanced skeleton visualization for view invariant human action recognition," *Pattern Recognition*, vol. 68, pp. 346–362, 2017.
- [7] M. Liu, F. Meng, C. Chen, and S. Wu, "Joint dynamic pose image and space time reversal for human action recognition from videos," in *Proceedings of the AAAI Conference on Artificial Intelligence*, vol. 33, no. 01, 2019, pp. 8762–8769.
- [8] S. Yan, Z. Li, Y. Xiong, H. Yan, and D. Lin, "Convolutional sequence generation for skeleton-based action synthesis," in *Proceedings of the IEEE/CVF International Conference on Computer Vision*, 2019, pp. 4394–4402.
- [9] R. Li, S. Yang, D. A. Ross, and A. Kanazawa, "Ai choreographer: Music conditioned 3d dance generation with aist++," in *Proceedings of the IEEE/CVF International Conference on Computer Vision*, 2021, pp. 13 401–13 412.
- [10] S. Ginosar, A. Bar, G. Kohavi, C. Chan, A. Owens, and J. Malik, "Learning individual styles of conversational gesture," in *Proceedings of the IEEE/CVF Conference on Computer Vision and Pattern Recognition*, 2019, pp. 3497–3506.
- [11] U. Bhattacharya, E. Childs, N. Rewkowski, and D. Manocha, "Speech2affectivegestures: Synthesizing co-speech gestures with generative adversarial affective expression learning," in *Proceedings of the 29th ACM International Conference on Multimedia*, 2021, pp. 2027–2036.
- [12] Y. Hou, H. Yao, X. Sun, and H. Li, "Soul dancer: Emotion-based human action generation," *ACM Transactions on Multimedia Computing, Communications, and Applications (TOMM)*, vol. 15, no. 3s, pp. 1–19, 2020.
- [13] M. Petrovich, M. J. Black, and G. Varol, "Action-conditioned 3d human motion synthesis with transformer vae," in *Proceedings of the IEEE/CVF International Conference on Computer Vision*, 2021, pp. 10 985–10 995.
- [14] P. Cervantes, Y. Sekikawa, I. Sato, and K. Shinoda, "Implicit neural representations for variable length human motion generation," in *European Conference on Computer Vision*. Springer, 2022, pp. 356–372.
- [15] C. Guo, X. Zuo, S. Wang, X. Liu, S. Zou, M. Gong, and L. Cheng, "Action2video: Generating videos of human 3d actions," *International Journal of Computer Vision*, vol. 130, no. 2, pp. 285–315, 2022.
- [16] Y. Yuan and K. Kitani, "Dlow: Diversifying latent flows for diverse human motion prediction," in *European Conference on Computer Vision*. Springer, 2020, pp. 346–364.
- [17] F. G. Harvey, M. Yurick, D. Nowrouzezahrai, and C. Pal, "Robust motion in-betweening," *ACM Transactions on Graphics (TOG)*, vol. 39, no. 4, pp. 60–1, 2020.
- [18] Y. Duan, T. Shi, Z. Zou, Y. Lin, Z. Qian, B. Zhang, and Y. Yuan, "Single-shot motion completion with transformer," *arXiv preprint arXiv:2103.00776*, 2021.
- [19] E. Barsoum, J. Kender, and Z. Liu, "Hp-gan: Probabilistic 3d human motion prediction via gan," in *Proceedings of the IEEE conference on computer vision and pattern recognition workshops*, 2018, pp. 1418–1427.
- [20] L.-Y. Gui, Y.-X. Wang, X. Liang, and J. M. Moura, "Adversarial geometry-aware human motion prediction," in *Proceedings of the European Conference on Computer Vision (ECCV)*, 2018, pp. 786–803.
- [21] A. Davydov, A. Remizova, V. Constantin, S. Honari, M. Salzmann, and P. Fua, "Adversarial parametric pose prior," in *Proceedings of the IEEE/CVF Conference on Computer Vision and Pattern Recognition*, 2022, pp. 10 997–11 005.
- [22] G. Pavlakos, V. Choutas, N. Ghorbani, T. Bolkart, A. A. Osman, D. Tzionas, and M. J. Black, "Expressive body capture: 3d hands, face, and body from a single image," in *Proceedings of the IEEE/CVF conference on computer vision and pattern recognition*, 2019, pp. 10 975–10 985.
- [23] S. Peng, Y. Zhang, Y. Xu, Q. Wang, Q. Shuai, H. Bao, and X. Zhou, "Neural body: Implicit neural representations with structured latent codes for novel view synthesis of dynamic humans," in *Proceedings of the IEEE/CVF Conference on Computer Vision and Pattern Recognition*, 2021, pp. 9054–9063.
- [24] G. Tiwari, D. Antić, J. E. Lenssen, N. Sarafianos, T. Tung, and G. Pons-Moll, "Pose-ndf: Modeling human pose manifolds with neural distance fields," in *European Conference on Computer Vision*. Springer, 2022, pp. 572–589.
- [25] J. Kim, J. Kim, and S. Choi, "Flame: Free-form language-based motion synthesis & editing," *arXiv preprint arXiv:2209.00349*, 2022.
- [26] S. Raab, I. Leibovitch, P. Li, K. Aberman, O. Sorkine-Hornung, and D. Cohen-Or, "Modi: Unconditional motion synthesis from diverse data," *arXiv preprint arXiv:2206.08010*, 2022.
- [27] E. J. Findlay, H. Zhang, Z. Chang, and H. P. Shum, "Denoising diffusion probabilistic models for styled walking synthesis," *arXiv preprint arXiv:2209.14828*, 2022.
- [28] M. Zhang, Z. Cai, L. Pan, F. Hong, X. Guo, L. Yang, and Z. Liu, "Motiondiffuse: Text-driven human motion generation with diffusion model," *arXiv preprint arXiv:2208.15001*, 2022.
- [29] G. Tevet, S. Raab, B. Gordon, Y. Shafir, D. Cohen-Or, and A. H. Bermano, "Human motion diffusion model," *arXiv preprint arXiv:2209.14916*, 2022.
- [30] I. Goodfellow, J. Pouget-Abadie, M. Mirza, B. Xu, D. Warde-Farley, S. Ozair, A. Courville, and Y. Bengio, "Generative adversarial networks," *Communications of the ACM*, vol. 63, no. 11, pp. 139–144, 2020.
- [31] D. P. Kingma and M. Welling, "Auto-encoding variational bayes," *arXiv preprint arXiv:1312.6114*, 2013.
- [32] M. Loper, N. Mahmood, J. Romero, G. Pons-Moll, and M. J. Black, "Smpl: A skinned multi-person linear model," *ACM transactions on graphics (TOG)*, vol. 34, no. 6, pp. 1–16, 2015.
- [33] J. Ho, A. Jain, and P. Abbeel, "Denoising diffusion probabilistic models," *Advances in Neural Information Processing Systems*, vol. 33, pp. 6840–6851, 2020.
- [34] A. Q. Nichol and P. Dhariwal, "Improved denoising diffusion probabilistic models," in *International Conference on Machine Learning*. PMLR, 2021, pp. 8162–8171.
- [35] P. Dhariwal and A. Nichol, "Diffusion models beat gans on image synthesis," *Advances in Neural Information Processing Systems*, vol. 34, pp. 8780–8794, 2021.
- [36] C. Guo, S. Zou, X. Zuo, S. Wang, W. Ji, X. Li, and L. Cheng, "Generating diverse and natural 3d human motions from text," in *Proceedings of the IEEE/CVF Conference on Computer Vision and Pattern Recognition*, 2022, pp. 5152–5161.
- [37] S. Saadatnejad, A. Rasekh, M. Mofayez, Y. Medghalchi, S. Rajabzadeh, T. Mordan, and A. Alahi, "A generic diffusion-based approach for 3d human pose prediction in the wild," *arXiv preprint arXiv:2210.05669*, 2022.
- [38] B. Degardin, J. Neves, V. Lopes, J. Brito, E. Yaghoubi, and H. Proença, "Generative adversarial graph convolutional networks for human action synthesis," in *Proceedings of the IEEE/CVF Winter Conference on Applications of Computer Vision*, 2022, pp. 1150–1159.
- [39] J. Sohl-Dickstein, E. Weiss, N. Maheswaranathan, and S. Ganguli, "Deep unsupervised learning using nonequilibrium thermodynamics," in *International Conference on Machine Learning*. PMLR, 2015, pp. 2256–2265.
- [40] O. Ronneberger, P. Fischer, and T. Brox, "U-net: Convolutional networks for biomedical image segmentation," in *International Conference on Medical image computing and computer-assisted intervention*. Springer, 2015, pp. 234–241.
- [41] J. Ho and T. Salimans, "Classifier-free diffusion guidance," *arXiv preprint arXiv:2207.12598*, 2022.
- [42] A. Shahroudy, J. Liu, T.-T. Ng, and G. Wang, "Ntu rgb+d: A large scale dataset for 3d human activity analysis," in *Proceedings of the IEEE conference on computer vision and pattern recognition*, 2016, pp. 1010–1019.
- [43] S. Park, D.-K. Jang, and S.-H. Lee, "Diverse motion stylization for multiple style domains via spatial-temporal graph-based generative model," *Proceedings of the ACM on Computer Graphics and Interactive Techniques*, vol. 4, no. 3, pp. 1–17, 2021.
- [44] D. P. Kingma and J. Ba, "Adam: A method for stochastic optimization," *arXiv preprint arXiv:1412.6980*, 2014.